Mössbauer-effect study of the Morin transition and atomic positions in hematite under pressure

C. L. Bruzzone* and R. Ingalls
Department of Physics, University of Washington, Seattle, Washington 98195
(Received 2 August 1982; revised manuscript received 13 January 1983)

The Mössbauer spectrum of hematite (α-Fe_2O_3) has been investigated over a range of pressures extending to 53 kbar and at temperatures ranging from 77 to 340 K. Particular attention has been paid to the effects of the Morin (spin-flip) transition on the ^{57}Fe quadrupole splitting. The anomalous reduction in the quadrupole splitting at points in P-T space near the Morin transition is explained by the application of magnetic anisotropy energy-density arguments, which also yield the mean magnetic-domain size in hematite. From the low-temperature quadrupole-splitting data and knowledge of the pressure dependence of the Morin temperature rather precise information concerning the location of atoms within the unit cell can be extracted. These results are in agreement with the latest high-pressure x-ray diffraction work. In addition, the hyperfine magnetic field is found to increase discontinuously by 1.5% through the pressure-induced Morin transition, similarly to the temperature-induced transition at atmospheric pressure. By taking advantage of recent advances in high-pressure technology and consistently applying the anisotropy energy-density theory of the Morin transition due to Artman, Murphy, and Foner, we have explained all of the features of our data, as well as the anomalies in previous work.

I. INTRODUCTION

The Morin spin-flip transition in hematite (α-Fe_2O_3) consists of antiferromagnetically coupled ferric ions rotating from the rhombohedral [111] axis for $T < T_M$, the Morin temperature ($\sim$260 K), to within 10^{-5} degrees of the (111) plane for higher temperatures.[1] Since the spins are puckered by $\sim 10^{-3}$ degrees from the planes of mirror symmetry for $T > T_M$, there is a small net magnetization perpendicular to [111] which disappears[2] below T_M. While much work has gone into understanding this transition and showing the magnetization to be consistent with the magnetic symmetry group of hematite,[3] there has been no satisfactory theory to explain both the ambient and the high-pressure hematite data.[4,5] Previous high-pressure work has been incompatible with the otherwise satisfactory theory of the Morin transition developed by Artman, Murphy, and Foner (the AMF theory),[6] which appears consistent with the small particle work of Kundig *et al.*,[7] Yamamoto,[8] and Schroeer and Nininger[9] and the effects of impurity substitutions for ferric ions,[10–12] as well as properly predicting the value of T_M in pure hematite.[6]

The verification of the AMF theory by means of small particle studies is based on the fact that hematite particles with dimensions less than 80 nm exhibit an expansion in lattice constants, and the AMF theory can be used to predict the effects of changing lattice constants upon the Morin temperature (Sec. III). However, the AMF theory is based on summations of dipole-dipole interactions which extend $6A$ in all directions, where A ($\simeq$0.5 nm) is the basal plane lattice constant.[6] This means that, for ferric ions within $\sim$3 nm of the surface, the AMF theory is clearly inappropriate. For a 60-nm-diam particle, for instance, about $\frac{1}{4}$ of the cations are in an environment not predicted by the AMF theory. The quantitative application of the AMF theory to particles of this size is probably not justified.

The impurity substitution work of Besser *et al.*,[10] Tasaki and Iida,[11] and Galasso and Williamson[12] is also difficult to interpret. In the AMF theory the Morin transition results from a competition between anisotropy energy densities (AED's) arising from crystal field-spin orbit interactions (K_{FS}), and the anisotropic distribution of magnetic dipoles (K_{MD}). Owing to the nature of these terms, K_{FS} is sensitive to the local crystal environment through its dependence on the crystalline field, while K_{MD} is dependent upon the long-range distribution of magnetic cations. In their analysis, Besser *et al.*[10] expect that K_{MD} will decrease with x, the fraction of ferric ions replaced by impurities. While this is undoubtedly true for large values of x, it is not obvious *a priori* for small x. Dipoles within (111) planes are all ferromagnetically coupled, meaning that their dipolar fields oppose the dipole alignment within the plane. Adjacent planes are similarly ferromagnetic, but an-

tiferromagnetically coupled to the original plane, thus their dipolar fields support the alignment of dipoles in the reference plane. Given the nature of dipole-dipole interactions and the magnetic symmetry of hematite, the loss of a single magnetic ion from an otherwise normal hematite lattice could result in a destabilization of the high-temperature configuration over the low-temperature one. This is identical in effect to an increase in K_{MD}. Calculations to determine the actual effect of removing one ferric ion have not been performed, however, the dipolar magnetic field has been shown to augment the molecular field in the low-temperature configuration and oppose the molecular field in the high-temperature configuration[13] (see also the experimental results of this work). This raises serious doubts as to the validity of the arguments used in previous impurity substitution work.

The least ambiguous approach to testing the AMF theory would be a direct variation of the lattice constants for large particles without lattice distortion. The experiment which should most nearly approximate this sort of variation is the application of hydrostatic pressure. When high-pressure Mössbauer[4] and neutron-diffraction[5] experiments were performed, however (as will be addressed in Sec. III), the data were in apparent conflict with the AMF theory. As interpreted by Worlton *et al.*[14] and Worlton and Decker,[15] these data would require pressure-dependent higher-order terms in the free-energy expansion[15]

$$F=\tfrac{1}{2}K\cos^2\theta+\tfrac{1}{2}K_1'\cos^4\theta + K_2'\cos\theta\sin^3\theta\sin\phi-K_3'\sin^2\theta + K_4'\cos6\phi\sin^6\theta\ , \tag{1}$$

where θ is the angle the dipole makes with the [111] axis, and ϕ is the angle with respect to a $\langle 2\bar{1}\bar{1}\rangle$ direction. The sharpness of the Morin transition at $P=0$ and the excellent agreement of the theoretical and experimental values[6] for T_M suggest that the K_i' are all negligible at zero pressure. (K_4' is nonzero, giving rise to the spin-canting which produces the weak ferromagnetism above T_M, but it is $\sim 10^{-6}K$ according to Besser *et al.*)[10] If the K_i' become large under pressure, the AMF theory will become invalid. Besser and Decker[15] state that their pressures in excess of 10 kbar are not hydrostatic. This pressure coincides nicely with the onset of effects which are not compatible with the AMF theory in the neutron-diffraction data.[15] Similar nonhydrostatic effects may be present in the Vaughan and Drickamer data. While it is not clear what effect the nonhydrostatic pressure will have on the Morin transition, uniaxial stress along the C axis is known to affect K_4' quite strongly.[10] It is therefore quite likely that nonhydrostatic pressures may produce anomalous changes in $K=K_{\mathrm{MD}}+K_{\mathrm{FS}}$. Furthermore, the hematite particle size in these experiments was not measured. In view of the previously described effects of particle size this question could be quite important. Finally, none of the previous high-pressure work considered the possibility of relaxation effects near the Morin transition. It will be shown in Secs. III and V that these effects are crucial for a proper understanding of the room-temperature high-pressure Mössbauer and neutron-diffraction data.

For the above reasons, we have reexamined the experimental and theoretical aspects of high pressure on the magnetism in hematite.

II. HEMATITE STRUCTURE

The structure of hematite may be described in either rhombohedral or hexagonal coordinates. The rhombohedral coordinate system (dashed lines in Fig. 1) is described by a rhombohedral length a, and angle α, while the hexagonal coordinates are A and C (the basal and axial hexagonal distances). The relationship between these systems is expressed in terms of the angle γ (Fig. 1), by

$$A=\sqrt{3}\,a\sin\gamma\ , \tag{2}$$

$$C=3a\cos\gamma\ . \tag{3}$$

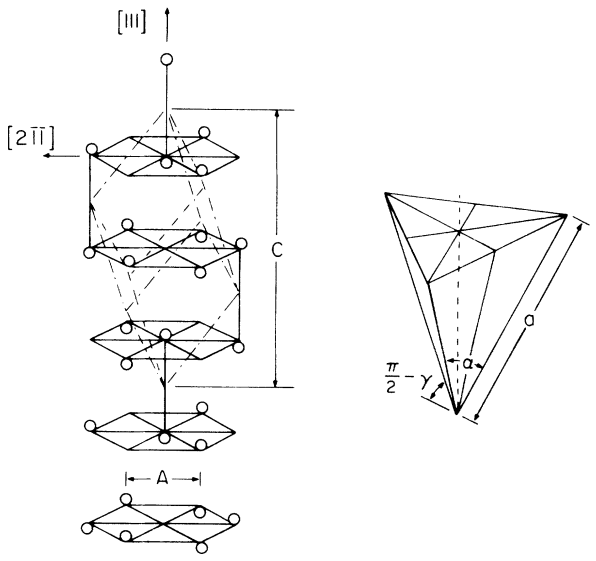

FIG. 1. Relationship between rhombohedral (dashed lines) and hexagonal unit cells may be derived from this figure. Using $\gamma=\arctan(2/\sqrt{3}\sin\alpha/2)$, the hexagonal coordinates may be obtained from $A=\sqrt{3}\,a\sin\gamma$ and $C=3a\cos\gamma$, where a and α are the rhombohedral side length and angle, respectively. Only ferric ions are shown for clarity.

The currently accepted zero-pressure values for A and C are[16] 0.5038(2) and 1.3772(12) nm. The fractional coordinates of the atoms in the rhombohedral unit cell are given by Fe^{3+} at $\pm[w\,w\,w]$ and $[(1\pm w)(1\pm w)(1\pm w)]$, and oxygens at $[u\,-u\,0]$, $[(\frac{1}{2}-u)(u+\frac{1}{2})\frac{1}{2}]$, and cyclic permutations. In hexagonal coordinates, the ferric ions are positioned along the C axis at $\pm 3wC$ and $3C(1\pm w)$. The oxygen ions are at a radius of uA from the C axis, with those in the $C=0$ plane rotated $-30°$ from each of the three basal plane axes (the $\langle 2\bar{1}\bar{1}\rangle$ axes in the rhombohedral system), and those at $\frac{1}{2}C$ rotated by $+30°$ from the basal axes. The currently accepted values for u and w under ambient conditions[16] are 0.3059(10) and 0.1053(1). The origin used in this description is at the center of an Fe_2O_3 "pseudomolecule," and is the most commonly chosen origin.

III. THEORETICAL AND EXPERIMENTAL BACKGROUND

The AMF theory[6] for the Morin transition is based upon the magnetic anisotropy energy-density (magnetic AED) work of Tachiki and Nagamiya.[17] This work shows that there are two dominant AED's which determine the magnetic axes of hematite and isomorphic compounds. These are the magnetic-dipole AED, $K_{MD}(P,T)$, and the fine-structure (sometimes called single-ion) AED, $K_{FS}(P,T)$.

$K_{MD}(0,0)$ is an easily calculated quantity arising from the dipole-dipole interactions between each magnetic cation and its anisotropically distributed neighbors. It may be calculated from[6]

$$K_{MD}(0,P)=\tfrac{3}{4}\rho n^2\mu_B^2 \times\sum_i P_i(3\cos^2\theta_i-1)/R_i^3 , \quad (4)$$

n representing the number of Bohr magnetons per ion, ρ as the number of ions per cm^3, μ_B as the Bohr magneton, P_i symbolizing the orientation of the ith dipole ($+1$ or -1), and R_i,θ_i specifying the location of ith dipole with respect to the reference ion. $K_{FS}(0,0)$, however, originates from the spin-orbit interaction coupled with the interaction between the orbital angular momentum and the crystalline field.[17] To date, K_{FS} has not proven tractable to calculation from first principles or to direct measurement. While measurements of K_{FS} as a function of pressure have been performed for compounds isologous to hematite,[18] questions of precision and pertinence to the current problem make any conclusions drawn, tentative at best. The fact that no variation in K_{FS} for Cr^{3+}-doped Al_2O_3 was observed below 50 kbar (Ref. 18) is at least consistent with the assumption that K_{FS} is constant up to this pressure. The variation occurring above 50 kbar raises questions as to the validity of the assumption beyond that point, however, it may be due to the generation of nonuniform stresses within the nonhydrostatic pressure medium. Impurity substitutions[10–12] suggest that K_{FS} is sensitive to distortions of the crystal lattice, but insensitive to isotropic changes in the lattice constants. This is important as it suggests that K_{FS} will not be appreciably affected by the application of hydrostatic pressure.

To evaluate $K_{FS}(0,0)$, Artman *et al.*[6] measured the net AED $K=K_{FS}+K_{MD}$ using antiferromagnetic resonance, then calculated K_{MD} from Eq. (4), thereby inferring K_{FS}. When the temperature dependence of K_{FS} and K_{MD} are calculated in the molecular field approximation, the results are[6,17]

$$K_{MD}(P,T)=K_{MD}(P,0)B_J(x) , \quad (5)$$

$$K_{FS}(P,T)=K_{FS}(P,0)\{2(S+1) -3B_J(x)\coth[x/(2S)]\} \times[1/(2S-1)] , \quad (6)$$

$$x=[3S/(S+1)](T_N/T)B_J(x) , \quad (7)$$

$$B_J(x)=(1/J)\{(J+\tfrac{1}{2})\coth[(J+\tfrac{1}{2})x] -\tfrac{1}{2}\coth(x/2)\} , \quad (8)$$

where $J=\frac{5}{2}$ for the ferric ions. These equations yield the temperature behavior shown in Fig. 2. When K_{MD} is evaluated,[6] it is found to be less than zero. From Fig. 2 it is seen that K_{MD} dominates in the temperature range above T_M, aligning the spins in the proper direction to explain the Morin transition. Moreover, since changes in the lattice constants simply change R_i and θ_i in Eq. (4), the effects of these changes are calculable (Fig. 3).

At the iron sites in hematite there is an electric field gradient directed along the [111] axis. This means that the Mössbauer-effect quadrupole-interaction energy E_Q, which behaves as

$$E_Q(\theta)=E_Q(0)(\tfrac{3}{2}\cos^2\theta-\tfrac{1}{2}) , \quad (9)$$

should change from $-\frac{1}{2}E_Q(0)$ to $E_Q(0)$ if the temperature is lowered or the pressure raised through the Morin transition phase boundary in P-T space (Fig. 4). When Vaughan and Drickamer[4] varied the pressure for a room-temperature hematite sample, they observed the behavior shown in Fig. 5. In order to explain this unexpected behavior, they considered the effects on $E_Q(0)$ of varying the iron and oxygen special position parameters w and u (Fig. 6). This led them to postulate a decrease in w of about 3% by 30 kbar, which would result in $E_Q(0)$ becoming 0 mm/sec at that pressure. However, since the

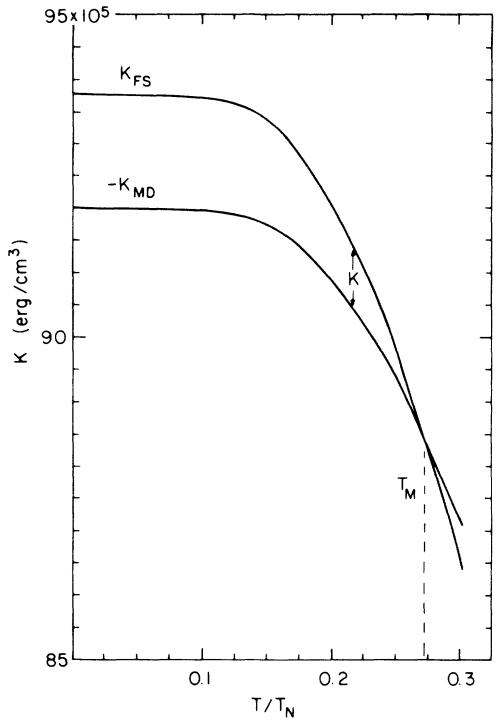

FIG. 2. Temperature variation of K_{MD}, K_{FS}, and K. The Morin transition is shown to occur when $K=0$ in this figure. It is likely that $K+K_{ME}$, where K_{ME} is the contribution due to magnetoelastic effects, must become zero in actuality.

ferric ions within a pseudomolecule are in two face-sharing coordination octahedra (in violation of the Pauling rules),[19] they repulse one another strongly as is evidenced by the departure of the cations from the octahedral centers at $w=\frac{1}{8}$. This repulsion would make a decreasing w with pressure unlikely. Also, the fact that $\partial T_M/\partial P>0$ requires (given the known variation of A and C with pressure) that w increase with pressure if the AMF theory is correct (Fig. 3). It also seems unreasonable to expect w to change so rapidly with pressure. What were not considered in the analyses of these data were any relaxation effects due to the proximity of the Morin transition, and the possibility that the hematite particles used might be too small to be considered bulk hematite. The second possibility would result in an anomalously high Morin transition pressure [due to lowering of $T_M(P=0)$ with decreasing particle size[7–9]], as well as anomalously small values for $E_Q(0)$, both of which were observed. (Vaughan and Drickamer[4] quote a Morin pressure of ~ 30 kbar as opposed to the 15 kbar suggested by Fig. 4, and a value of $E_Q(0)$ of 0.7 mm/sec, as opposed to 0.84 mm/sec quoted elsewhere.[7])

In considering spin-relaxation effects near $T_M(P)$, the rate at which relaxation occurs is crucial.[20] Calculations of the superparamagnetic relaxation time τ as a function of the magnetic anisotropy energy have been done.[7] It is to be expected that spin-flip transitions will occur on a time scale similar to or less than τ. In hematite, τ is short compared to the decay time for the 14.4-keV excited state in the ^{57}Fe nucleus, but long compared to the nuclear procession time. In this case a normal statistical mechanical average over the spin directions may be performed. For a two-level system with $\theta=\theta_1$ and θ_2 separated by an energy difference D (cf. Ref. 21),

$$\langle E_Q\rangle=\frac{E_Q(\theta 1)+E_W(\theta_2)e^{D/kT}}{1+e^{D/kT}}\ . \tag{10}$$

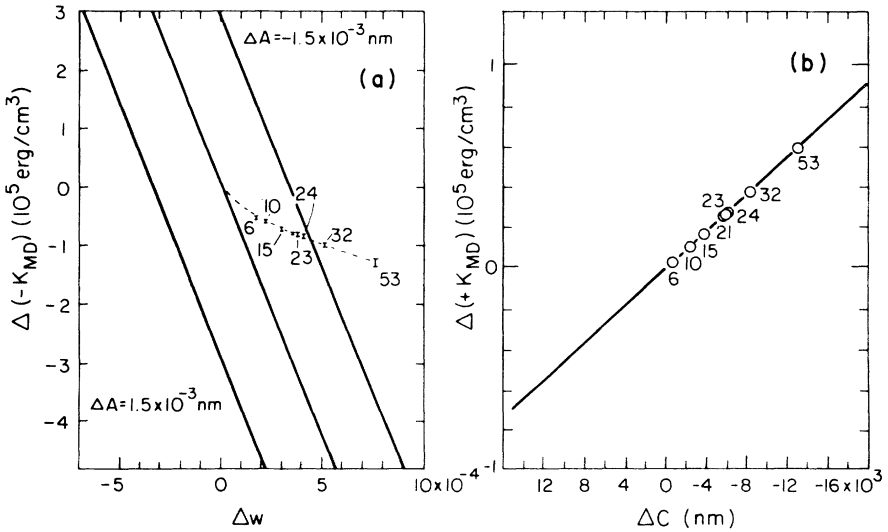

FIG. 3. Relationship between (a) ΔK_{MD}, Δw, and ΔA, and (b) ΔK_{MD} and ΔC. Numbered points correspond to pressures at which these parameters were determined.

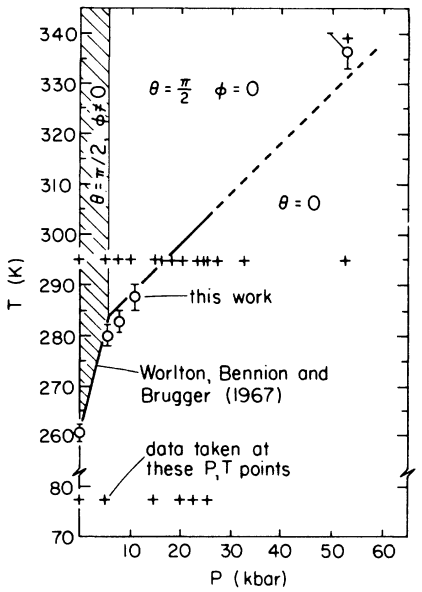

FIG. 4. Magnetic phase diagram of hematite. θ and ϕ are the axial and azimuthal angles between the [111] axis and spins. In the cross-hatched region, the magnetization is nonzero. It vanishes in a second-order manner when entering the $\theta=\pi/2$, $\phi=0$ region, and in a first-order fashion between $\theta=\pi/2$ and $\theta=0$. The boundary between $\theta=\pi/2$ and $\theta=0$ denotes the Morin transition line.

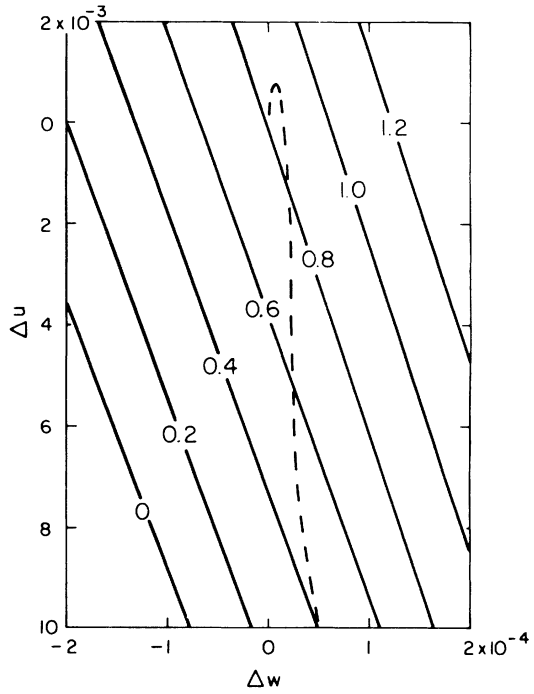

FIG. 6. Variation of $E_Q(0)$ with the oxygen and iron special parameters u and w after Ref. 4. Dashed line represents the pressure dependence from the present work.

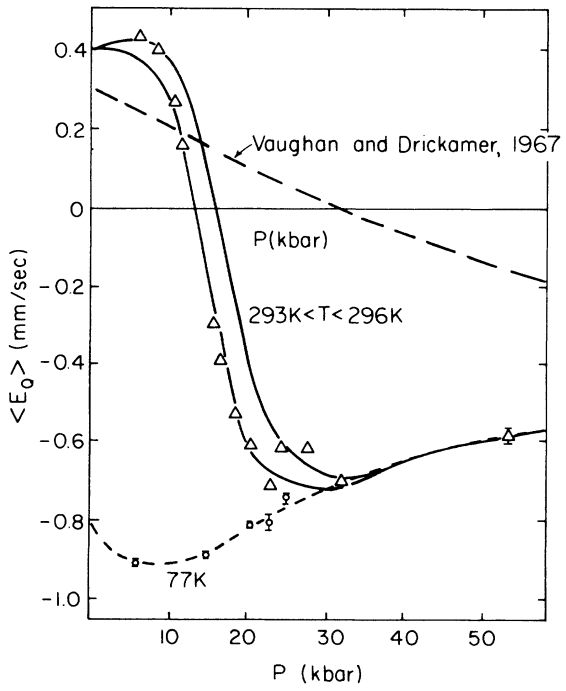

FIG. 5. Quadrupole interaction E_Q vs pressure as measured by Vaughan and Drickamer (Ref. 4) (dashed line) and in this work. Solid lines are the results of a theoretical fit to the room-temperature data taking relaxation phenomena into account. At 200 kbar the Vaughan and Drickamer data had reached −0.50 mm/sec.

For hematite, $\theta_1=\pi/2$ and $\theta_2=0$, so

$$E_Q(\theta_1)=-\tfrac{1}{2}E_Q(0)\,, \tag{11a}$$

$$E_Q(\theta_2)=E_Q(0)\,. \tag{11b}$$

In Sec. VI, D will be calculated from

$$D=Kv+K_{\mathrm{ME}}v\,, \tag{12}$$

where K_{ME} is included to account for magnetoelastic effects. In his consideration of these effects, Searle demonstrated that they can explain much of the low-pressure variation of T_M with pressure.[22] The pressure at which the magnetoelastic interaction disappears (due to the vanishing of the spin-canting angle ϕ in the basal plane) is given by[22]

$$P_c=\frac{H_D^2 M}{H_M}\frac{E}{P_0}\,, \tag{13}$$

where P_0 is the ambient pressure, H_D is the effective spin-canting field, M is the sublattice magnetization, H_M is the effective molecular field, and E is the elastic modulus of hematite. Since H_D is due to superexchange anisotropy[23] it would not be expected to be sensitive to temperature. The fact that the spontaneous magnetization persists to the Néel temperature is evidence for this. M and H_M should be proportional, so it would be expected that

$$\frac{1}{P_c}\frac{\partial P_c}{\partial T}\sim\frac{1}{E}\frac{\partial E}{\partial T}\ . \tag{14}$$

Using the logarithmic derivative of E for Al_2O_3,[24] one obtains the approximate result (in kbar/K)

$$\frac{\partial P_c}{\partial T}\simeq -0.02\ . \tag{15}$$

The second-order spin-canting transition line determined by this value is indicated in Fig. 4.

IV. EXPERIMENTAL TECHNIQUES

Data were taken using a moving-source, pressurized-absorber system[25] modified to accept clamp-type diamond anvil cells. Pressures were determined using the ruby fluorescence[26] technique. The pressure cells used were specially designed by us to minimize the effects of changing temperature upon the clamped pressure.[27] Pressure determination was done at temperatures down to 100 K on a specially designed fluorescence manometer system[28] in order to measure any residual changes in pressure with temperature. Any changes occurring from 300 to 100 K were extrapolated to the temperature of interest, should it be less than 100 K. Total pressure changes by 77 K were always less than ± 2 kbar.

Mössbauer spectra have been taken at the temperatures and pressures shown in Fig. 4. By taking data at points remote from the expected Morin transition in P-T space, spin-relaxation effects can be avoided. A second set of measurements are taken near the Morin transition so that differences from the first set of data indicate the effects of spin relaxation. In addition to constant-acceleration spectra, thermal scans[29] were taken at 0, 6, 8, and 11 kbar to verify the $\partial T_M/\partial P$ data of Worlton *et al.*[5]

Constant-acceleration data were analyzed using a least-squares program FLDFIT (Ref. 30) built around the synthetic spectrum routines of Gabriel and Ruby.[31] This program solves the Mössbauer Hamiltonian exactly for a given set of Mössbauer parameters, then varies the parameters to find a best fit to the raw Mössbauer spectrum. Three parabolic background parameters, the peak widths, the magnetic field, the electric field gradient magnitude, asymmetry, and axial and azimuthal angles, the recoilless fraction, and the isomer shift for each of three sets of nuclear environments could be simultaneously varied for the fit to each spectrum. In this work only one nuclear environment with an axially symmetrical electric field gradient was found to be necessary. Once this was verified for a few spectra, the search was restricted accordingly.

Thermal scan spectra were analyzed by taking the ratio of the count rate at an appropriately chosen resonant velocity to that at a nonresonant velocity and noting changes in this ratio as the temperature is changed. A rapid change indicates that a resonant velocity peak has moved to (or away from) the chosen velocity. In this work, such a change is indicative of the Morin transition temperature T_M at whatever pressure is being studied. All Morin temperatures were evaluated for increasing temperature, due to the thermal hysteresis in this transition.[32]

V. RESULTS AND ANALYSIS

An electron micrograph[33] of the hematite powder used in this work shows a mean particle size of about 90 nm, large enough to avoid "small particle" effects.[7–9] The results of Mössbauer-effect measurements on this sample are shown in Figs. 5, 7, and 8. The isomer shift E_I (Fig. 7), as a function of pressure, is in agreement with the results of Vaughan and Drickamer.[4] This is expected since particle size has very little effect on E_I.[4,7] As in the Vaughan and Drickamer results, the change in E_I with pressure is what is calculated from the expected second-order Doppler shift in the Debye model.[4] The change in E_I with temperature between 293 and 77 K [0.103(10) mm/sec] is also in agreement with Debye-model calculations (0.110 mm/sec) for a Debye temperature[33] of 600 K. The absence of changes in E_I not attributable to the second-order Doppler shift strongly suggests that the covalency of the bonds in hematite is not changing with pressure over the range of pressures studied.

Measurements of the magnetic field H (Fig. 8) show no change with pressure except for an abrupt increase of about 6 kOe at $P\cong 15$ kbar. A similar change in H noted at $T_M(0)$ by Tobler *et al.*[13] has been attributed to the change in the dipolar magnet-

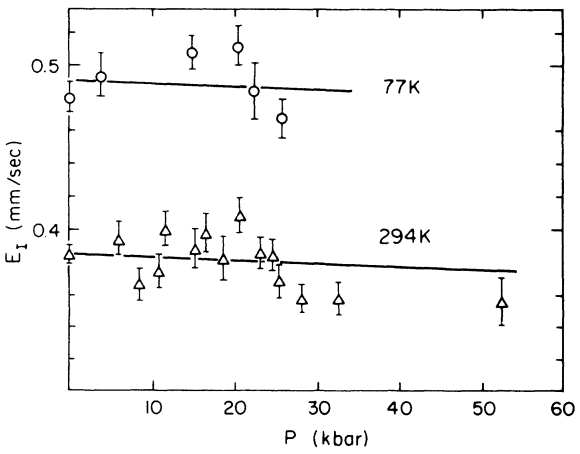

FIG. 7. Isomer shift relative to α iron E_I vs pressure. The lines indicate Debye-model results with $\Theta_D=600$ K.

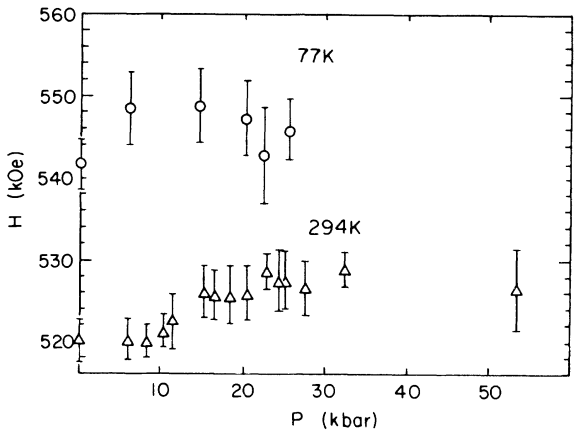

FIG. 8. Magnetic field at the iron nucleus vs pressure. The jump in H at ~ 15 kbar is due to a change in the dipolar field contribution of the other cations when they flop to the low-temperature configuration.

ic field produced by the neighboring ferric ions when they change orientation. It is not surprising that such an effect would be substantially independent of whether the Morin transition is induced by changing pressure or temperature.

Mössbauer measurements of $T_M(P)$ are shown in Fig. 4, along with the results of the $\partial T_M/\partial P$ measurements of Worlton *et al.*[5] The Mössbauer thermal-scan measurements lack the precision of the neutron-diffraction data used in Ref. 5, but were taken to confirm the behavior of $\partial T_M/\partial P$ with pressure. The 53-kbar measurement of T_M was not taken via the thermal-scan technique, and will be discussed below.

The most striking results occur in the quadrupole-interaction data (Fig. 5). It is clear that these results differ qualitatively from those of Vaughan and Drickamer,[4] and that E_Q varies from $-\frac{1}{2}E_Q(0)$ to $E_Q(0)$ as the pressure is raised. There is still a good deal of sluggishness to this transition; however, it may be explained quantitatively using the AMF theory.[6] In order to do so, $K_{\rm MD}(P,0)$ is first calculated from the observed variation of T_M/T_N with pressure, where T_N is the Néel temperature of hematite. It is clear from Fig. 2 that the temperature at which $K_{\rm MD}$ and $K_{\rm FS}$ intersect determines $K_{\rm MD}(P,0)$, provided $K_{\rm FS}(P,0)$ is assumed not to vary with pressure. [Actually, the invariance of $K_{\rm FS}(P,0)$ is not crucial to the argument that follows. The behavior of $K(P,T)$ is quite insensitive to the overall magnitude of $K_{\rm MD}$ and $K_{\rm FS}$.] The value of T_N used in the determination of $K_{\rm MD}$ is 961 K at zero pressure, and is assumed to increase by 1.4(1) K/kbar as the pressure is raised.[35] Having determined $K_{\rm MD}(P,0)$ from $T_M(P)$, $K(P,T)$ is known for all temperatures from Eqs. (5)—(7). The only quantity needed to solve Eqs. (10)—(12) for $\langle E_Q \rangle$ for all pressures is the magnetic-domain volume v. In order to evaluate v, the value of $\langle E_Q \rangle$ at 10.4 kbar and 294 K is used in conjunction with the appropriate value for D/v, and Eqs. (10)—(12) are solved for v. This result for v is then used with the values of $K_{\rm MD}(P,T)$ at all other pressures to find $\langle E_Q \rangle$ at T for those pressures. The solid lines in Fig. 5 indicate the maximum and minimum values for $\langle E_Q \rangle$ with $v=4750(10)$ nm^3, $\Delta T_M(P)=1.0$ K, an absorber temperature fluctuation of ± 1.5 K, and the uncertainties indicated by the error bars for the measurements of $E_Q(0)$ at 77 K. The fits to the data are quite satisfactory. The AED, and therefore $\langle E_Q \rangle$ is very sensitive to the temperature of the absorber. Much of the apparent scatter in the room-temperature data is due to uncontrolled fluctuations in the ambient temperature of the laboratory. From Eqs. (10) and (11) it can be seen that at the Morin transition $\langle E_Q \rangle = \frac{1}{4}E_Q(0)$. The E_Q data therefore imply a Morin pressure at room temperature $P_M=14.5(5)$ kbar. When analyzed in this way, the data of Vaughan and Drickamer yield values of 70(5) kbar. Assuming $\partial T_M \partial/P$ is unaffected by particle size, this latter result would imply a zero-pressure value for T_M of ~ 210 K compared to the bulk value of 260 K. This and the extreme sluggishness of their transition is consistent with a domain volume of 500(100) nm^3.

At this point the assumption that $\tau \ll 98$ nsec should be checked. The results of calculations (after Ref. 7) are shown in Fig. 9 for $v=4750$ nm^3. These results indicate that $\tau \ll 98$ nsec except when $K \lesssim 10^4$ erg/cm^3; i.e., when the Morin transition is approached quite closely. This explains why just at the Morin transition two distinct six-line spectra

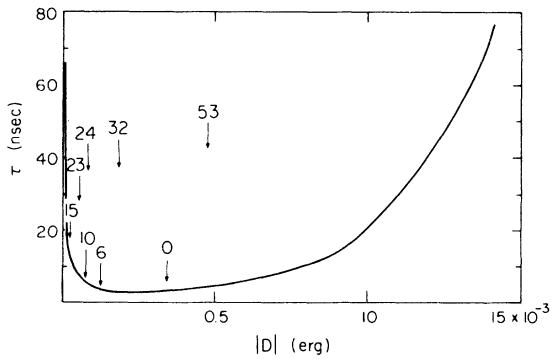

FIG. 9. Superparamagnetic relaxation time vs the spin-alignment energy. $\tau \ll 98$ nsec implies that the Mössbauer nucleus sees a time-averaged angle θ between the magnetic axis and the principal axis of the electric-quadrupole tensor. Numbered points correspond to the pressures at which the data were taken.

may be observed.[36] In this case (when $D \simeq 0$) $\tau \gg 98$ nsec and only one spin configuration is apparent to the Mössbauer nucleus.

The procedure followed above for explaining the sluggishness in the quadrupole interaction at the Morin transition can also be reversed to provide a technique for finding $T_M(P)$. In order to do this, a constant-acceleration Mössbauer spectrum is taken far from that temperature (e.g., 77 K). The value of $E_Q(0)$ at pressure, P, determined by the second spectrum is placed in Eq. (10), as is the measured value for $\langle E_Q \rangle$ near $T_M(P)$. Since v has previously been determined, a value for $K(P,T)$ is obtained. Since K has a well-known temperature dependence, the value of $T_M(P)$ needed to make $D=0$ is easily determined. The 53-kbar point for T_M in Fig. 4 has been determined in this way.

VI. CRYSTALLOGRAPHIC IMPLICATIONS

Having shown the AMF theory to be consistent with high-pressure Mössbauer-effect measurements, it is reasonable to attempt to determine atomic positions in hematite as functions of pressure using this information. The AMF theory and a knowledge of $\partial T_M/\partial P$, $A(P)$, and $C(P)$ is adequate to determine $w(P)$, the iron special position parameter. [The lattice parameters $A(P)$ and $C(P)$ have recently been measured quite accurately by Finger and Hazen.[37]] Since $T_M(P)$ has been shown (above) to yield $K_{MD}(P,0)$, changes in $w(P)$ may be determined from Fig. 3. The resulting behavior of $\Delta w(P)$ is shown in Fig. 10.

It was mentioned in Secs. I and III that magnetoelastic effects probably account for much of the low-pressure variation in $T_M(P)$. A consideration of this effect by Searle[22] indicates that it accounts for about 10 K of the variation in T_M by 5.6 kbar. Since the magnetoelastic effect requires the presence of a nonzero basal plane magnetization, it disappears at 5.6 kbar when the spin-canting angle goes to zero.[22] The coincidence of this pressure with the change in $\partial T_M/\partial P$ (Fig. 4) is evidence for the validity of Searle's treatment. Such effects are included in the following consideration.

Since the AMF theory neglects the basal plane anisotropy energy and magnetoelastic effects, the magnetoelastic energy density must be added to the value of K due to effects considered in the AMF theory. The magnetoelastic energy-density contribution (calculated at 6 kbar) is $\sim 0.27 \times 10^5$ erg/cm^3. The effects on $w(P)$ of adjusting all values of $K_{MD}(P,0)$ appropriately are shown in Fig. 10. The fact that w increases with pressure is consonant with the expectations outlined in Sec. III. When iron-iron distances along the [111] axis are calculated and

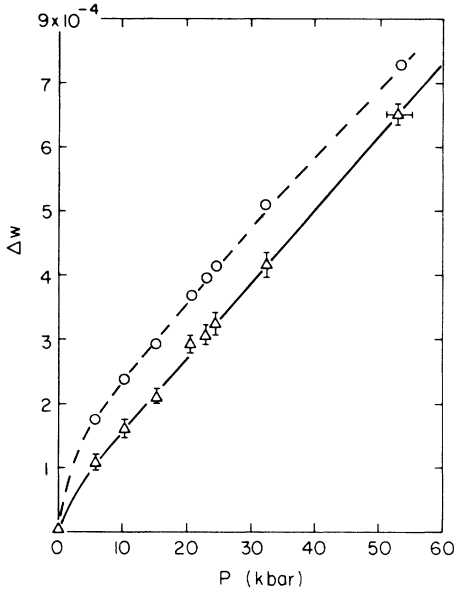

FIG. 10. Change in the iron special position parameter w with pressure. Circles indicate the results of the AMF theory (Ref. 6) without considering magnetoelastic effects, while triangles show the result of including magnetoelastic effects.

compared with those measured via single-crystal x-ray diffraction by Finger and Hazen[37] (Fig. 11), the results agree within the stated errors. The error bars on the present AMF measurements include estimates of all random and systematic errors *except* for those arising from any possible variations in K_{FS} with P, the possible effects of a non-negligible anisotropy in the superexchange interaction,[23] and deviations of the magnetoelastic effects from Searle's predictions.[22] While the agreement with Finger and Hazen is reasonably good, their data require w to decrease with pressure and are thus qualitatively different from ours.

It should be noted that the calculation of $\langle E_Q \rangle$ is unaffected by the addition of a magnetoelastic energy of the size required above ($\sim 0.3\%$) to K_{MD}. The value for the magnetic-domain volume v is also unaffected.

In order to determine changes in the oxygen special position parameter u with pressure the measured values of $E_Q(0)$ at pressure and the results for $\Delta w(P)$ determined above are used in conjunction with the calculations for $E_Q(0)$ as a function of u and w represented[4,38] in Fig. 6. The results for $\Delta u(P)$ are shown in Fig. 12.

Once $A(P)$, $C(P)$, $u(p)$, and $w(P)$ are all determined up to 53 kbar, all other interatomic distances may be determined. In particular, the two smallest iron—oxygen bond lengths may be calculated and compared with the x-ray measurements of Finger

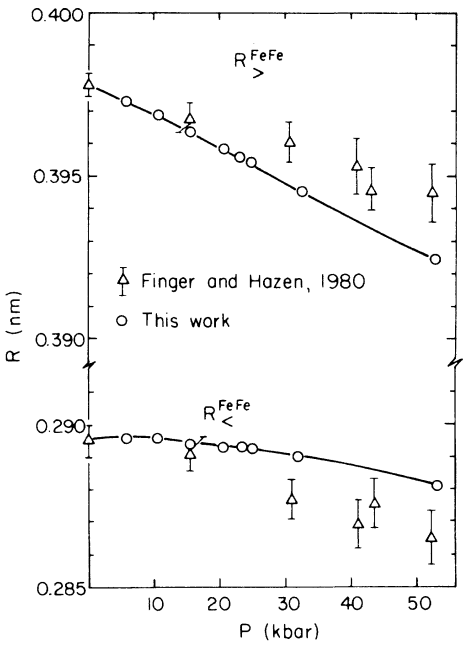

FIG. 11. Two smallest iron-iron distances along the [111] axis. The agreement with Finger and Hazen (Ref. 37) is acceptable. Quoted errors of Finger and Hazen have been doubled to give them the same meaning as the errors quoted in this paper, which are smaller than the data points unless specifically indicated.

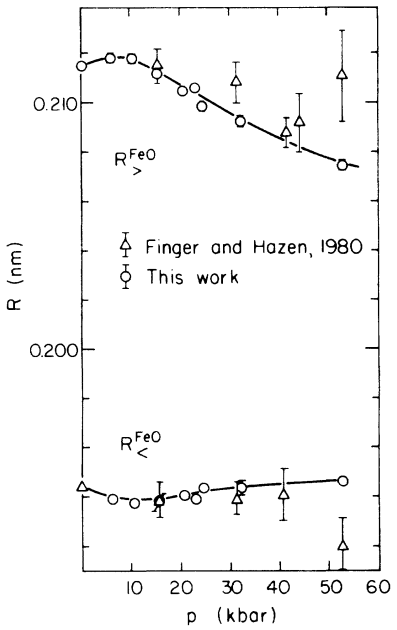

FIG. 13. Iron—oxygen bond lengths in hematite as a function of pressure. The agreement with Finger and Hazen (Ref. 37) is excellent except at 53 kbar. These data points are inconsistent with the systematic variations of the other data, and are probably in error.

and Hazen[37] (Fig. 13). Only the 53-kbar x-ray data differs dramatically from our measurement. These x-ray data, however, would require that one of the iron—oxygen bond lengths reverse its systematic (and expected) trend with pressure and rapidly return to its zero-pressure value at 53 kbar. Since the iron-iron and iron-oxygen distance determinations require precision x-ray intensity measurements from a sample inside a diamond anvil cell, it is likely that this anomalous variation is due to unexpected changes in the x-ray attenuation at higher pressures.

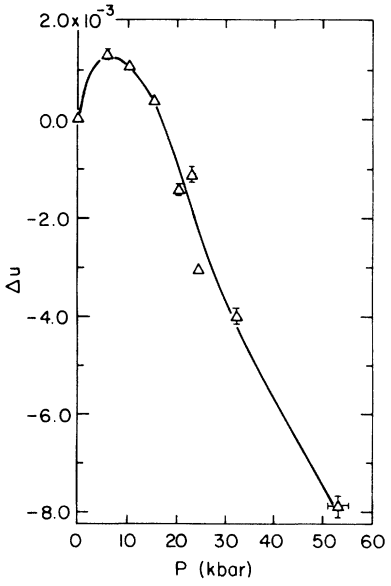

FIG. 12. Oxygen special position parameter u vs pressure. This variation assumes magnetoelastic effects at low pressure as described by Searle (Ref. 22).

VII. CONCLUSIONS

High-pressure Mössbauer-effect data have been shown to be in quantitative agreement with the anisotropy energy-density theory of Artman, Murphy, and Foner[6] for the Morin transition. Measurements of the quadrupole-interaction energy and Morin temperature as a function of pressure have been used to determine the average magnetic-domain size in hematite, which is found to be 4750(10) nm^3 for bulk hematite.

If the variation with pressure of $K_{FS}(P,T)$ is assumed to be negligible, the change in $K_{MD}(P,0)$ with pressure may be obtained from measurements of $T_M(P)$. With the use of the values so obtained for $K_{MD}(P,0)$ and the results of magnetoelastic calculations by Searle,[22] changes in the iron special position parameter w with pressure have been calculated. The results for $\Delta w(P)$ have been used in conjunction with calculations of the quadrupole interaction as a function of u and w and measurements of the quadrupole-interaction energy to determine $\Delta u(P)$, the change in the oxygen special position parameter

with pressure. The resulting iron—oxygen bond lengths are found to be in agreement with those determined by x-ray diffraction.[37]

The quadrupole interaction has also been used to determine $T_M(P)$ from two constant-acceleration Mössbauer spectra, providing an alternative means for extending measurements of $T_M(P)$ to any desired pressure.

Isomer shift measurements in hematite indicate that the s electron density at the iron nucleus has not changed for pressures up to 53 kbar. This suggests that the Sternheimer antishielding factor and the covalency of the atomic bonds are not changing in this pressure range, as any changes in the $3d$ electron states would affect the screening of the s electrons. The lack of any change in the magnetic field with pressure (other than the expected 6-kOe change at P_M due to changing dipolar fields) supports this inference.

ACKNOWLEDGMENTS

The authors wish to thank J. Artman, L. Finger, and R. Hazen for discussing these results and making helpful suggestions. We also wish to thank L. Galasso and D. Williamson for permission to discuss their experimental results prior to publication. Finally, we would like to acknowledge the extensive assistance provided by R. Ralph and J. Whitmore throughout this work. This work was supported by the National Science Foundation Grant No. DMR 78-24995.

---

*Present address: 3M Center, Bldg. 201, St. Paul, MN 55144.

[1]P. J. Flanders, in *Magnetism and Magnetic Materials—1971, Chicago,* Proceedings of the 17th Annual Conference on Magnetism and Magnetic Materials, edited by C. D. Graham and J. J. Rhyne (AIP, New York, 1972), p. 795.

[2]T. Townsend Smith, Phys. Rev. 8, 721 (1916).

[3]I. Dzyaloshinsky, J. Phys. Chem. Solids 4, 241 (1958).

[4]R. W. Vaughan and H. G. Drickamer, J. Chem. Phys. 47, 1530 (1967).

[5]T. G. Worlton, R. B. Bennion, and R. M. Brugger, Phys. Lett. 24A, 653 (1967).

[6]J. O. Artman, J. C. Murphy, and S. Foner, Phys. Rev. 138A, 912 (1965).

[7]W. Kundig, H. Bommel, G. Constabaris, and R. H. Lindquist, Phys. Rev. 142, 327 (1966).

[8]Naoichi Yamamoto, J. Phys. Soc. Jpn. 24, 23 (1968).

[9]D. Schroeer and R. C. Nininger, Jr., Phys. Rev. Lett. 19, 632 (1967).

[10]P. J. Besser, A. H. Morrish, and C. W. Searle, Phys. Rev. 153, 632 (1967).

[11]A. Tasaki and S. Iida, J. Phys. Soc. Jpn. 16, 1697 (1961).

[12]Lin Galasso and D. Williamson (private communication).

[13]L. Tobler, W. Kundig, and P. F. Meier, Berichte der Fruehj. Schw. Phys. Ges. 53, 257 (1980).

[14]Actually, Worlton *et al.* (Ref. 5) made an error in sign in their analysis and did not note the wrong sign of $\partial T_M/\partial P$. They were concerned with explaining the sign of $\partial^2 T_M/\partial P^2$; however, their approach could also be applied to $\partial T_M/\partial P$.

[15]T. G. Worlton and D. L. Decker, Phys. Rev. 171, 596 (1968).

[16]R. L. Blake, R. E. Hessevick, T. Zoltai, and L. W. Finger, Am. Mineral. 51, 123 (1966).

[17]Masashi Tachiki and Takeo Nagamiya, J. Phys. Soc. Jpn. 13, 452 (1958).

[18]D. R. Stephens and H. G. Drickamer, J. Chem. Phys. 35, 427 (1961).

[19]L. Pauling, *The Nature of the Chemical Bond,* 2nd ed. (Cornell University Press, Ithaca, New York, 1948), p. 396ff.

[20]M. Blume and T. A. Tjon, Phys. Rev. 165, 446 (1968); 165, 456 (1968).

[21]H. Shechter, J. G. Dash, G. A. Erickson, and R. Ingalls, Phys. Rev. B 2, 613 (1970).

[22]C. W. Searle, Phys. Lett. 25A, 256 (1967).

[23]Toru Moriya, Phys. Rev. Lett. 4, 228 (1960).

[24]N. Soga and O. L. Anderson, J. Am. Ceram. Soc. 49, 239 (1967).

[25]C. M. Liu and R. Ingalls, Rev. Sci. Instrum. 49, 1680 (1978).

[26]J. D. Barnett, S. Block, and G. J. Piermarini, Rev. Sci. Instrum. 44, 1 (1973).

[27]J. E. Whitmore, C. L. Bruzzone, and R. Ingalls, *High Pressure in Research and Industry* (8th AIRAPT Association Internationale for Research and Advancement of High Pressure Science and Technology and 9th EHPRG European High Pressure Research Group Conferences), edited by C. M. Backman, T. Johannisson, and L. Tegnér (Arkitektkopia, Uppsala, Sweden, 1982), p. 579.

[28]J. E. Whitmore, C. L. Bruzzone, and R. Ingalls, Rev. Sci. Instrum. 53, 1602 (1982).

[29]D. G. Howard, B. D. Dunlap, and J. G. Dash, Phys. Rev. Lett. 15, 628 (1965).

[30]Copies of this program available upon request.

[31]J. R. Gabriel and S. L. Ruby, Nucl. Instrum. Methods 36, 23 (1965).

[32]R. C. Nininger and D. Schroeer, J. Phys. Chem. Solids 39, 137 (1978).

[33]Electron micrograph courtesy of D. Brownlee, University of Washington, Department of Astronomy.

[34]F. Gronvold and E. F. Westrum, J. Am. Chem. Soc.

81, 1780 (1958).
[35]D. Bloch, Ann. Phys. (Paris) 1, 93 (1966); used in conjunction with measurements of $\partial V/\partial P$ from Ref. 37.
[36]Kazuo Ono and Atsuko Itô, J. Phys. Soc. Jpn. 17, 1012 (1962).
[37]Larry W. Finger and Robert M. Hazen, J. Appl. Phys. 51, 5362 (1980).
[38]Includes corrections of the original calculation (Ref. 4) according to the results of J. O. Artman, A. H. Muir, and H. Wiedersich, Phys. Rev. 173, 337 (1968).